



University of Bahrain
**Journal of the Association of Arab Universities for
Basic and Applied Sciences**

www.elsevier.com/locate/jaaubas
www.sciencedirect.com



Mesoporosity, thermochemical and probabilistic failure analysis of fired locally sourced kaolinitic clay



Muazu Abubakar^a, Uday Basheer^{b,c}, Norhayati Ahmad^{b,*}

^a Department of Mechanical Engineering, Bayero University, Kano, Nigeria

^b Faculty of Mechanical Engineering, Universiti Teknologi Malaysia, Skudai, Johor Bahru, Malaysia

^c Centre for Low Carbon Transport in Cooperation with Imperial College London, Institute for Vehicle Systems and Engineering, Universiti Teknologi Malaysia, Skudai, Johor, Malaysia

Received 9 November 2016; revised 5 March 2017; accepted 14 April 2017

Available online 29 May 2017

KEYWORDS

Characterization;
Mullite;
Flexural strength;
Mesopores;
Weibull distribution

Abstract A dense and mesoporous ceramic from locally sourced Nigerian clay under fracture-strength test were produced and the reliability analysis of the fractured strength was conducted using a three-parameter Weibull probability distribution. The samples were prepared by addition of starch (0–20wt%), pressed at 60 MPa and fired at 1300 °C. The as-received Nigerian clay, dense and porous ceramic were characterized using XRD, XRF, TGA/DTA, PSD, multi-point BET and FESEM. The fracture strength of the samples (33 each) was determined using a three-point bending test. The fracture strength data were analyzed using three-parameter Weibull probability distribution. From the characterization results, a mullite ceramic formed at a sintering temperature of 1300 °C. The threshold strength for the three-parameter Weibull provides the strength below which the dense and the porous ceramic will not fail. The Weibull moduli of the ceramics at different starch compositions show that failure modes in these materials are not identical. The Weibull modulus increases with increase in percentage starch from 0% to 15%. However, the value decreases with 20% starch addition. Reliability analysis provides a detailed interpretation and assessment of the fracture strength of the porous ceramics.

© 2017 University of Bahrain. Publishing services by Elsevier B.V. This is an open access article under the CC BY-NC-ND license (<http://creativecommons.org/licenses/by-nc-nd/4.0/>).

1. Introduction

Due to the rising cost of engineering ceramics and the limitations of polymeric membranes with regard to mechanical,

chemical and thermal properties, researchers have resorted to using inexpensive clay minerals in ceramic membrane production for industrial processes such as reaction, separation and purification applications (Mauricio et al., 2011; Bose and Das, 2013; Emani et al., 2014). These clay minerals can be a cheap source of mullite ceramic, which can be obtained after sintering at the appropriate temperature (Bai, 2010). Despite the availability of literature on the strength data of these porous fired clay materials, a detailed analysis of the strength and

* Corresponding author.

E-mail addresses: muazumani2004@yahoo.com (M. Abubakar), nhayati@fkm.utm.my (N. Ahmad).

Peer review under responsibility of University of Bahrain.

<http://dx.doi.org/10.1016/j.jaubas.2017.04.002>

1815-3852 © 2017 University of Bahrain. Publishing services by Elsevier B.V.

This is an open access article under the CC BY-NC-ND license (<http://creativecommons.org/licenses/by-nc-nd/4.0/>).

reliability of these materials is important, since they operate under pressure-based driven process. However, the strength and reliability of these porous fired clays are not well understood. As a rule-of-thumb, brittle materials have variations in their fracture strength under the same fabrication conditions; this is due to the fact that brittle materials are prone to flaws/pores during the fabrication process, which become pronounced after sintering. Many researchers have reported single fracture strength at a particular sintering temperature and compaction pressure as the actual strength of these clay-based porous materials. For example, porous clay based membranes were produced at a distributed pressure of 2 Kg and fired at temperatures in the range of 850–1000 °C; the membranes produced have fracture strength values in the range 3–8 (Nandi et al., 2008). In addition, Jana et al., 2010 reported a fracture strength of 11.55 at a sintering temperature of 1000 °C while preparing porous microfiltration membranes by paste casting for chromate removal from wastewater. Several years later, Yakub et al. (2012) extended the research by reporting the deviation of the fracture strength of porous fired clay at a sintering temperature of 955 °C with a porosity in the range 36–47%; the fracture strength obtained are in the range 3.89 ± 0.09 – 7.14 ± 2.26 MPa. Moreover, Sahnoun and Baklouti, 2013 reported strength in the range 6.66–10.63 for porous fired kaolin clay prepared by compaction at compaction pressure in the range of 15–75 at sintering temperature in the range 800–1250 °C. Lastly, Emani et al. (2013) reported the fracture strength of kaolin-based porous fired membrane using compaction at a pressure range of 29–49, firing temperature of 900–1000 °C and porosity in the range 35–39%; the fracture strength obtained is in the range 7.81–11.

Conventional two-parameter Weibull assumes the strength below which all the materials will not fail (threshold strength) to be zero and the scale parameter to be the strength at 62.3% of the materials. In addition, the two-parameter Weibull probability distribution is suitable for a small sample size of 20 and below (Roos and Stawarczyk, 2012). However, in reliability statistics, higher Weibull modulus value is an indication that the threshold strength is larger than zero and should not be ignored (Han et al., 2009). Therefore, three-parameter Weibull probability distribution gives a detailed reliability of the strength below which all the tested materials will not fail (threshold strength) and uniformity of the strength data in the form of Weibull modulus. This is normally achieved by testing the strength of several samples (normally around 30) under the same fabrication condition and analyzing the data with three-parameter Weibull probability distribution (Han et al., 2009). Although, many studies have reported the strength of porous fired clays, there is limited research on the analysis of the strength data using three-parameter Weibull distribution. Therefore, we report the fabrication of dense and mesoporous fired Nigerian clay with starch as a pore former, characterization of the clay and the mesoporous fired clay and the analysis of the fracture strength using three-parameter Weibull probability distribution. The novelty of this work is to determine the strength below which these clay-based membranes will not fail, determine the uniformity of the data and the effect of porosity on the Weibull modulus. No attempt has been made previously on characterization and flexural strength analysis of dense and mesoporous fired Nigerian clay. The objective of the present research was to conduct XRF, XRD, PSD, FESEM and BET multi-point of as-received,

dense and porous ceramics. The analysis of the fracture strength of the dense and porous ceramics was conducted by three-parameter Weibull probability distribution.

2. Materials and methods

2.1. Clay characterization

The as-received clay obtained locally from Kankara, Nigeria was screened through 50 µm sieve. Particle size analysis was carried out using Malvern particle mastersizer 2000. Mineralogical composition of the raw and fired clay (1000 and 1300 °C) was determined with Siemens Diffractometer D5000 equipment, Cu Kα (1.54056 nm) radiation, step size angle of 0.05°, scan rate of 2° in 2θ unit and scan range from 5 to 70°. The XRD data were analyzed using EVA software. The TGA/DTA analysis of the clay was carried out using PerkinElmer thermal analyzer at a heating temperature range of 50–1100 °C, heating rate of 10 °C/minute and flow rate of 20 ml/min under a nitrogen atmosphere.

2.2. Sample Preparation and characterization

The flexural strength samples were prepared from the raw clay and the clay mixed with 0, 10, 15 and 20% starch (label as A, B, C and D respectively in Table 1). The samples were compacted into a die of dimensions approximately 5 × 30 × 80 mm at a compaction pressure of 60 with an Instron 600 KN machine at 10 min holding time to attain perfect consolidation. Thirty three samples each were fabricated for the dense, 10, 15 and 20%. The samples were fired in a high temperature furnace at 1300 °C for a period of two hours. The flexural strength of samples A, B, C and D fired at 1300 °C (33 samples each) was determined using three point bending test. The specimens' width and breadth were measured and recorded and a span of 40 mm was used for the test. A load was applied on the specimen until fracture. The test was conducted using an Instron 100-KN electro-mechanical testing machine at a loading rate of 0.5 mm/min, based on the following equation (ASTM, 1999):

$$\sigma = \frac{3FL}{bd^2} \quad (1)$$

where σ is the flexural strength variable, F is the load, L is the span (40 mm), b is the width and d is the section thickness of specimen.

Multi-point BET was conducted on the dense porous ceramics at 1300 °C to determine the adsorption/desorption isotherm, average pore size and the pore size distribution on TriStarII 3020 surface area and pore analyzer with N₂ as adsorptive at –196 °C for 4 h in a vacuum. The morphology of the dense ceramic was recorded using Field Emission Scanning Electron Microscopy FESEM (ZEISS SUPRA35VP). For the porous ceramics, the samples were fractured, cold mounted, ground with 320–1200 grit of silicon carbide papers, polished using 1 µm diamond paste and cleaned with ultrasonic cleaner. The morphology was recorded with FESEM.

2.3. Three-parameter Weibull analysis

The fracture strength data were analyzed using three and two-parameter Weibull probability distribution with MINITAB 15

Table 1 Summary of flexural strength and three-parameter Weibull of A and porous sintered clay (B, C and D) based on three-parameter Weibull probability distribution.

Sample	Flexural strength (MPa)	m	S (MPa)	σ_0 (MPa)
A	24.11–46.56	2.56	19.05	16.11
B	13.58–23.26	3.12	11.17	7.27
C	9.99–15.30	3.28	8.21	4.61
D	3.06–12.65	2.15	1.78	6.33

software at 95% confidence interval (CI). The general cumulative three-parameter Weibull probability distribution for least square estimate (LS) is given by (Han et al., 2009):

$$P = 1 - \exp \left[- \left(\frac{\sigma - S}{\sigma_0} \right)^m \right] \quad (2)$$

where P is the probability of failure and σ_0 is the scale parameter, m is the Weibull modulus and S denotes the threshold (strength below which the material will not fail) (Naito, 2014a).

Taking twice the logarithm of Eq. (2) to obtain:

$$\ln [\ln(1/(1 - P))] = m \ln(\sigma - S) - m \ln(\sigma_0) \quad (3)$$

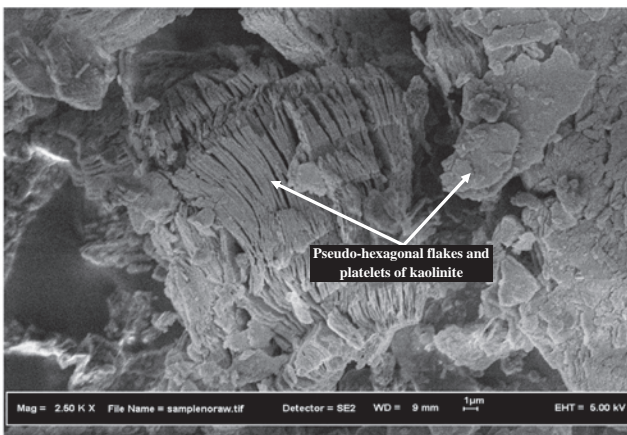
Eq. (3) is linear and when $\ln[\ln(1/(1 - P))]$ is plotted against $\ln(\sigma - S)$, a slope of m and an intercept of $-m \ln(\sigma_0)$ is obtained. Hence, the estimates of σ_0 , m and s are determined from the slope and intercept in Eq. (3). There are few ways of estimating the value of s . In this research, we employed the use of Minitab 15 software for estimating the Weibull parameters. For the two-parameter Weibull, $s = 0$ and Eq. (3) reduces to:

$$\ln[\ln(1/(1 - P))] = m \ln(\sigma) - m \ln(\sigma_0) \quad (4)$$

Probability of failure estimator (P) has to be assigned to estimate the probability of failure. The Hazen method (modified Kaplan Meier) has been used due to its least bias for $N \geq 20$ and probably the most preferable from a material science point of view (Naito, 2014b), given by:

$$P_i = \frac{R_i - 0.5}{N} \quad (5)$$

where R_i is the ranking position and N is the total number of samples.

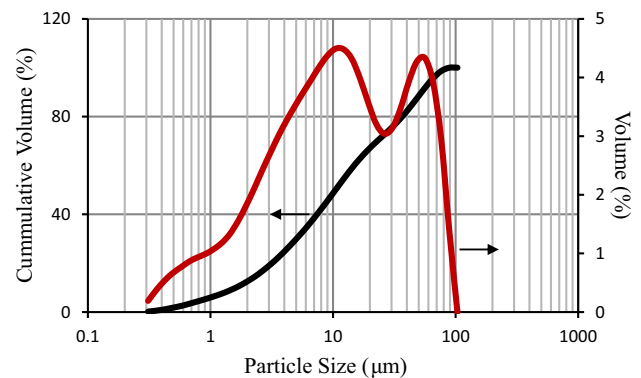
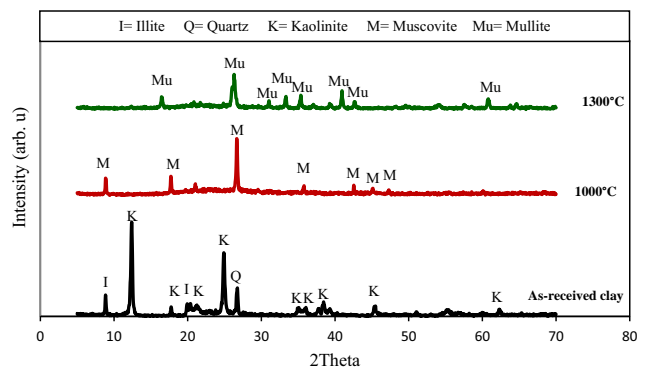
**Figure 1** FESEM morphology of as-received clay sieved through 50 μm .

3. Results and discussion

3.1. Raw material characterization

The morphology of the as-received clay Fig. 1 shows the presence of pseudo-hexagonal flakes of kaolinite in the form of accordion structure and platelets of kaolinite, this is a typical characteristic of kaolin clay. The particle size distribution of the clay (Fig. 2) shows a bimodal distribution with an average particle size of 22.46 μm . Other parameters obtained from the particle size analysis results are the specific surface area and the density, which are found to be 0.57 m^2/g and 2.56 g/cm^3 respectively.

The XRD analysis (Fig. 3) shows the presence of kaolinite (PDF-00-001-0527) as the predominant phase in the clay with trace of illite (PDF-00-058-5138) and quartz (PDF-00-058-2015) with percentages of 82.21%, 7.20% and 10.59%

**Figure 2** Particle size distribution of as received clay sieved through 50 μm .**Figure 3** XRD analysis of as-received clay and sintered samples at 1000 and 1300 $^{\circ}\text{C}$.

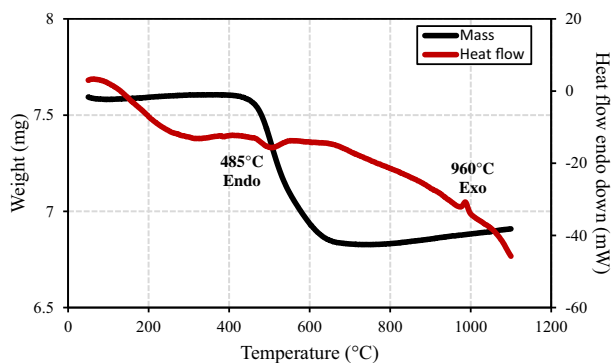


Figure 4 TGA/DTA analysis of as received Nigerian clay.

respectively; these are the phases normally found in kaolin clays (Gougazeh and Buhl, 2014). Sintering of the clay to a temperature of 1000 and 1300 °C. Fig. 3 shows the transformation of the clay. At a temperature of 1000 °C, it shows a distinct phase of muscovite (PDF-00-058-2037), while at sintering temperature of 1300 °C shows a well pronounced mullite phase (PDF-00-006-0258). The transformation of clays at various temperatures is heating rate dependent; heating rate of 3–20 °C/min is enough to cause the transformation of meta-kaolin to mullite without the formation of intermediate spinel phase (Castelein et al., 2001). The XRF chemical composition of the clay was found to be 48.86% SiO₂, 37.83% Al₂O₃, 1.15% K₂O, 0.27% Fe₂O₃, 0.05wt% CaO, 0.04% TiO₂, 0.04% MgO, 0.01% MnO, 0.01% P₂O₅ and 11.81% LOI (Abubakar et al., 2016).

Fig. 4 shows the decomposition of the clay with temperature. From the figure, the total weight loss of the clay is approximately 11.09% due to removal of both physical and chemical combined water, conversion of kaolin to metakaolin as supported by the DTA curve. The DTA curve shows an endothermic peak at a temperature of 485 °C; this is due to the conversion of kaolin to metakaolin and removal of chemically combined water. The second, an exothermic peak at a temperature of 960 °C; this is due to conversion of metakaolin to spinel.

3.2. Dense and porous ceramics characterization

The FESEM morphology of the dense ceramics at a sintering temperature of 1300 °C is shown in Fig. 5. The A sample ceramic shows a random distribution of micro cracks. However, the porous ceramics B and C (Fig. 6a and b) shows a partial and relative uniform distribution of slit-shaped pores respectively. However, Fig. 6c shows interconnection of pores in the form of cracks for porous ceramic D.

The pore size distribution and the adsorption/desorption isotherm obtained from the BET multi-point data of A, B, C and D are shown in Fig. 7. The adsorption/desorption isotherm of the dense ceramic Fig. 7a does not conform to any IUPAC standards for the identification of porous materials, which shows that the material is not porous or contains any appreciable amount of porosity. The adsorption/desorption isotherms of B, C and D show an initial increase in the adsorption isotherm due to monolayer formation and low slope region in the middle of the isotherm due to formation of first

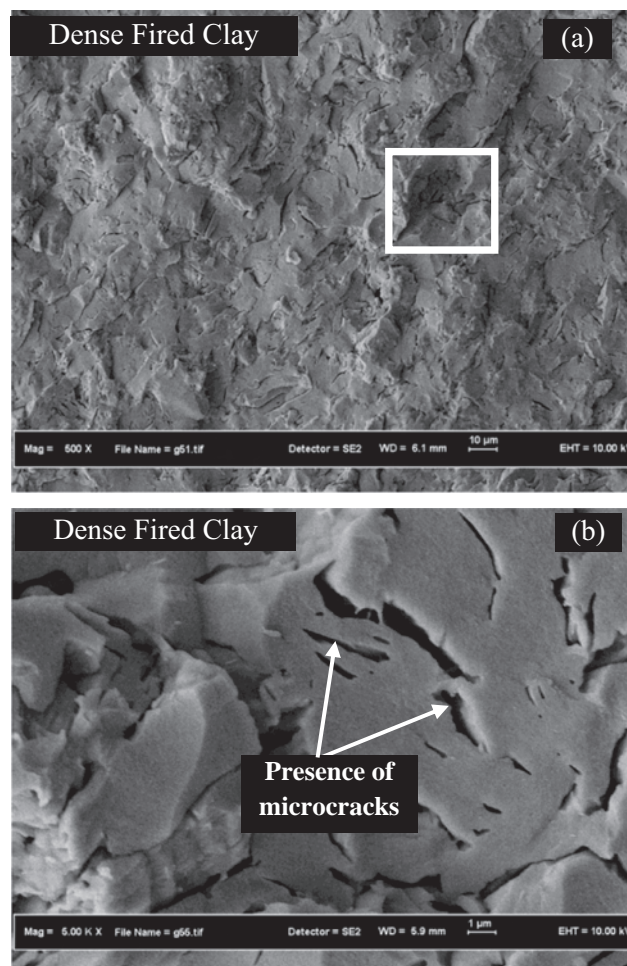


Figure 5 FESEM morphology of A sintered clay at 1300 °C (a) 500× and (b) 5000×.

multilayers, followed by a high increase in the adsorption amount of nitrogen at a relative pressure above 0.9 due to capillary condensation which further proves the presence of mesopores. The isotherm presents a step down in the desorption branch, with the desorption branch of the isotherm lying above the adsorption branch. According to IUPAC standards for the identification of porous materials, this behavior type is of type IV isotherm with H3 type hysteresis for all the porous ceramics produced (Fig. 7b, c and d). Presence of hysteresis of type H3 proved that the porous ceramics are mesoporous of slit-shaped pores. During the desorption process of the porous ceramics B and C, the isotherm closed at a relative pressure close to 0.1, which indicates a relative distribution of slit-shaped pores. The desorption isotherm of D does not close, which shows an interconnection of pores (Fig. 6c) and nitrogen gas retention in this pores during the desorption process, similar observation was reported by Schmitt et al., 2013. The pore size distribution shows all the porous ceramics contain a main sharp peak at approximately 20.00 nm, which are highly uniform in structure; other peaks are termed artificial peaks/troughs, which also contribute to the statistical thickness of the pores (Fu et al., 2010). The average pore size of B, C and D is found to be 39.68, 46.10 and 55.13 nm respectively, this further proves the porous ceramics are mesoporous. The

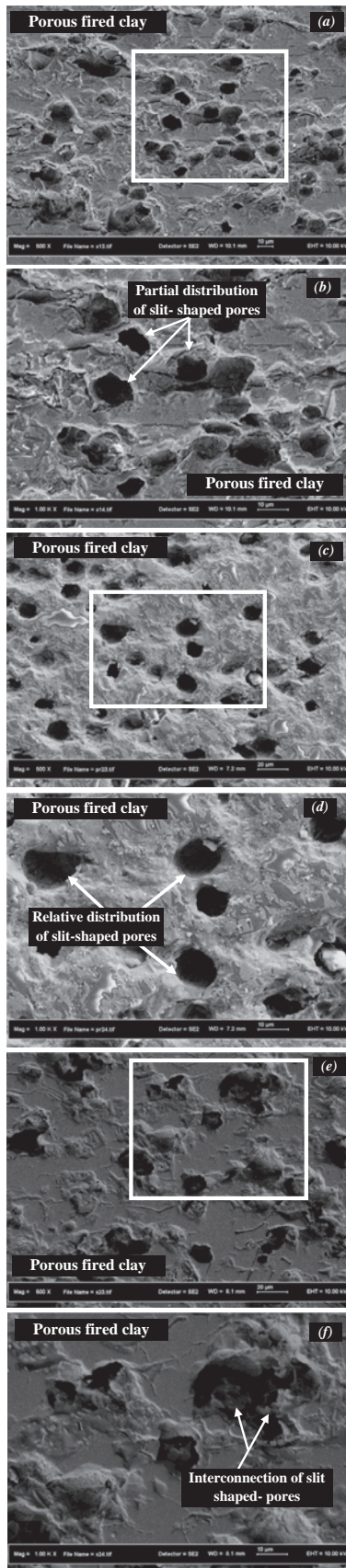


Figure 6 FESEM morphology of porous sintered clay with (a and b) sample B (c and d) sample C and (e and f) sample D.

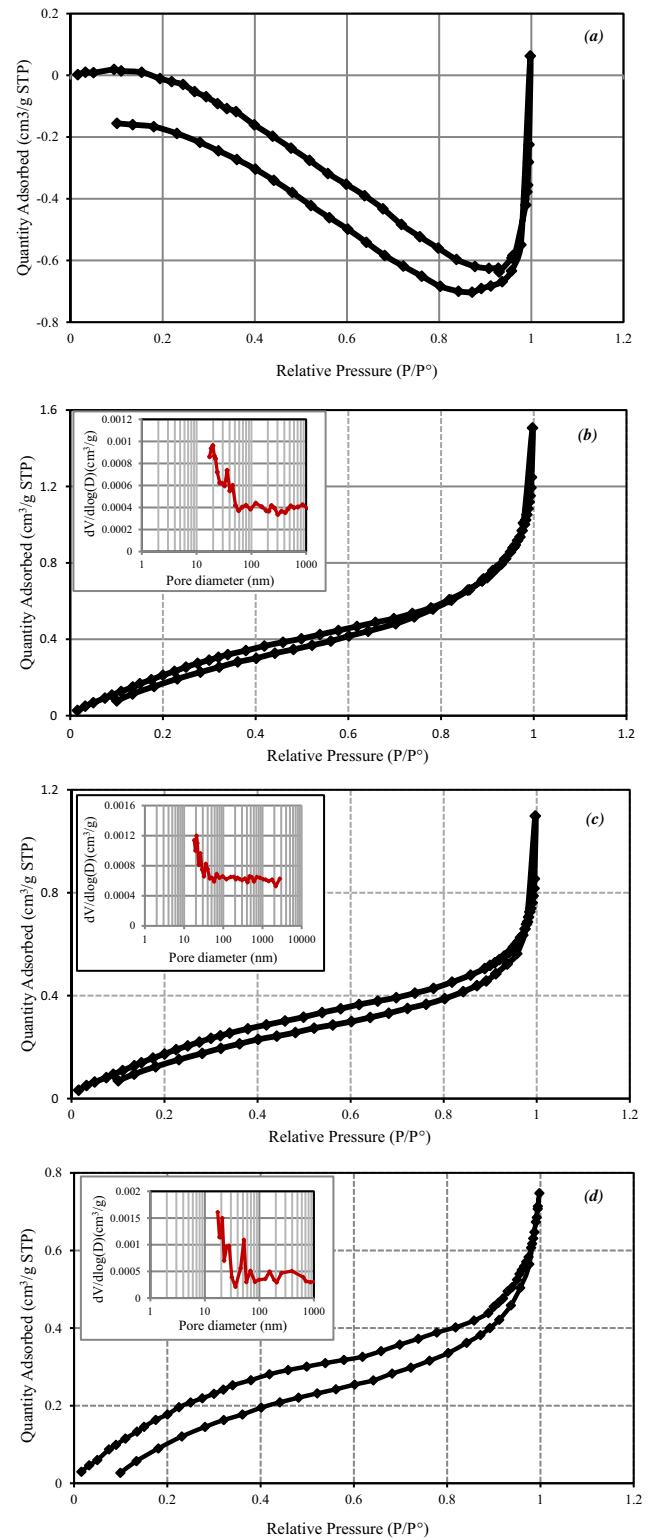


Figure 7 Adsorption/desorption isotherm and pore size distribution of (a) A, (b) B (c) C and (d) D.

BET specific surface area for the porous ceramics B, C and D was found to be 1.60, 2.11 and 3.63 m²/g respectively, this variation shows increase with increase in starch content, this is as a result of increase in porosity as percentage starch increases.

3.3. Reliability analysis three-parameter Weibull probability distribution

Table 1 shows the summary of the Weibull parameters of A, B, C and D. From the table, the Weibull modulus of C shows the highest value (3.28), this is due to uniform distribution of the slit shaped pores (Fig. 6b), while that of A Fig. 5 shows a value (2.56) due to the random distribution of cracks. In addition, the Weibull modulus of D shows the lowest value (2.15) among the porous ceramics. This is due to the interconnection of pores of random orientation, which reduces the uniformity of porosity in the porous ceramic (Fig. 6c). The threshold strength (the strength below which all the materials will not fail) shows decrease with increase in starch content from A, B, C and D. This is due to the increase of the pores, as the pore former burnt out during the sintering process, many voids are created, as a result, decreasing the strength of the ceramics. The probability plot Fig. 8 shows almost all the probability points lie within the upper and lower bounds of the 95% CI, which signifies the Hazen method of estimating the probability of failure, has fitted the fracture strength data for both dense and the porous ceramics. In Fig. 9, all the probability density plots skewed to the left i.e., toward the threshold strength. Also, from the probability density plot, it shows that C has the highest probability density, which shows that predicting failure is high compared with other compositions. High value of the Weibull modulus shows low spread of the fracture strength data, high uniformity/low variability and greater reliability. In engineering its more desirable to use materials with low strength but with higher reliability (Weibull modulus value) than materials with low high strength but lower reliability; since materials with higher Weibull modulus values are predictable and less likely to break at a stress value much lower than the mean value (Quinn and Quinn, 2010). The Weibull modulus value decreases as the percentage starch increases; this is due to the formation of interconnected pores (Fig. 5d), which resulted in non-uniform distribution of porosity. Sample A shows the smallest probability density; this can be attributed to the wider spread of the fracture strength data as shown in Fig. 8. In general, blunt flaws such as pores are less likely to cause failure than a sharp flaw such as microcracks; this supports the low Weibull modulus of the dense ceramic due to

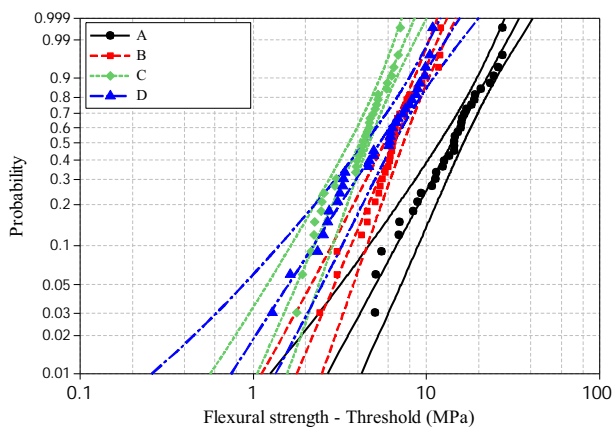


Figure 8 Probability plot of A and porous sintered clay (B, C, and D).

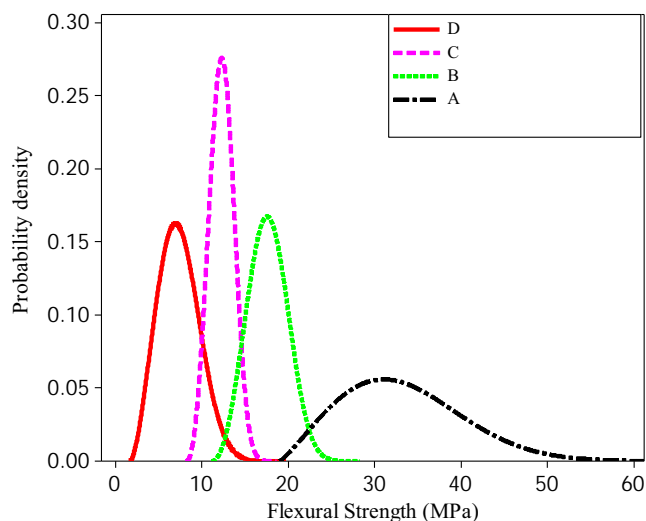


Figure 9 Probability density plot of A and porous sintered clay (B, C and D).

Table 2 Three-parameter Weibull of some engineering materials together with current research (Han et al., 2009).

Materials	m	S
PMMA-based bone cement	0.5–1.4	-
Window glass	1.21	35.8 MPa
Silicon die	2–3	48–184 MPa
Ti-6Al-4V	2.6	563 MPa
Titanium alloy 30NiCrMo16 steel	2.8	441 MPa
Cast iron ENGJS800-2	3.1	204 MPa
C20 Steel	3.2	230 MPa
Silicon nitride	3.6–4.5	389–506 MPa
Solid oxide fuel cells	~5	25–28 MPa
35NiCrMo4 steel	5.4	534 MPa
22NiMoCr37 ferritic steel	~7	2.4–3.2 GPa
ZuCuAl9Y) BMGs	6–6.8	1116–1677 MPa
This research (Samples A, B, C and D)	2.15–3.28	1.7–19.05 MPa

presence of microcracks as shown in Fig. 5. The Weibull modulus obtained from A, B, C and D are higher than other engineering materials (Table 2) as reported by Han et al., 2009.

3.3.1. Two-parameter Weibull probability distribution

Table 3 shows the summary of two-parameter Weibull distribution of A, B, C and D. From the Table, the Weibull modulus of B and C (9.52 and 10.10) is higher than that of A (6.58); D has the least value of the Weibull modulus. However, the scale parameter of A (35.75 MPa) is higher than B, C and D (18.62, 12.95 and 8.24 MPa respectively). In addition, the Weibull modulus C is higher than that of B. Conversely, the scale parameter of B is higher than that of C. This behavior of increase in Weibull modulus and decrease in scale parameter with increase in percentage starch in the porous ceramics is due to the fact that increase in starch from 10% to 15% results in more uniform distribution of porosity in C. While the decrease in scale parameter is due the high porosity content of C compared with B as shown in Fig. 6b. The two-

Table 3 Summary of two-parameter Weibull of dense and porous sintered clay (10, 15 and 20 wt% starch) based on three-parameter Weibull probability distribution.

Sample	m	σ_0 (MPa)
A	6.59	35.75
B	9.52	18.62
C	11.10	12.95
D	5.08	8.24

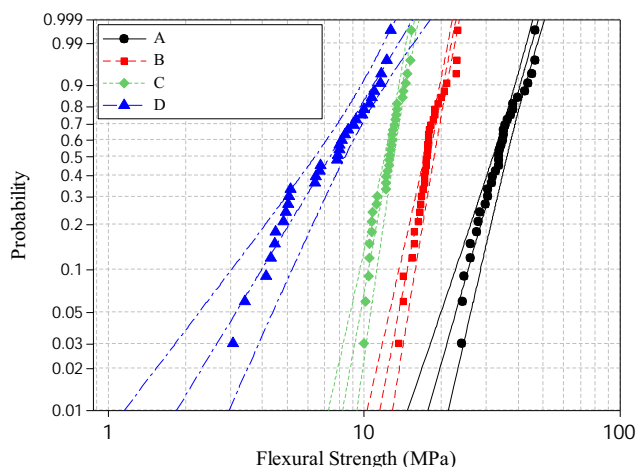


Figure 10 Two-parameter probability plot of A and porous sintered clay (B, C, and D).

parameter Weibull probability distribution using least square estimate at 95% confidence interval using Minitab software is shown in Fig. 10. The least square estimate of the two-parameter Weibull distribution does not fit well the data because in all the probability estimates, some points, which are more than 95% CI, lie outside the upper and lower bounds of the 95% confidence interval. The 95% confidence interval assumes that only 5% of the data point will lie outside the upper and lower bounds of the confidence interval.

For all the compositions, three-parameter Weibull threshold strength is less than the scale parameter of the two-parameter Weibull. This is due to the fact that the two-parameter Weibull considers failure at 63.2% of the tested specimens while the threshold strength in the case of the three-parameter Weibull considers the strength below which all the materials will not fail. The three-parameter Weibull provides the safety limit of the strength that should not be exceeded to avoid failure.

4. Conclusions

Porous mullite ceramic was obtained from low-cost clay from Nigeria. The Porous ceramics produced are mesoporous suitable for filtration applications. The porous membranes produced show an increase in Weibull modulus with an increase in uniform distribution of porosity. The produced membranes are mesoporous, which will find application in micro and ultra-filtration processes. The threshold strength obtained indicated the strength below which the materials will not fail under an applied pressure of micro and ultrafiltration applications. This

strength is very important since it provides the safe engineering limit which the porous ceramics will be subjected to without failure. It was also found that the Weibull modulus shows an increase in value with increased starch content from 10% to 15%, which signifies an increase in the distribution of porosity as shown in the micrographs. However, as percentage starch reaches 20wt%, the Weibull modulus decreases due to non-uniformity of porosity. The three-parameter Weibull provides the detailed safe limits of the ceramics produced.

Conflict of interest

The authors have no conflict of interest.

Acknowledgements

This research was sponsored by Universiti Teknologi Malaysia under contract research grant 4C044 and Ministry of Higher Education under FRGS Grant 4F552 and 4F808. Special thanks go to Bayero University Kano through Tertiary Education Training Fund (TETFund) for sponsoring the PhD program.

References

- Abubakar, M., Tamin, M.N., Saleh, M.A., Uday, M.B., Ahmad, N., 2016. Preparation and characterization of a nigerian mesoporous clay-based membrane for uranium removal from underground water. *Ceram. Int.* 42, 8212–8220.
- ASTM, Standard Test Methods for Flexural Properties of Ceramic Whiteware Materials, 1999, ASTM C674–88.
- Bai, J., 2010. Fabrication and properties of porous mullite ceramics from calcined carbonaceous kaolin and α -Al₂O₃. *Ceram. Int.* 36, 673–678.
- Bose, S., Das, C., 2013. Preparation and characterization of low cost tubular ceramic support membranes using sawdust as a pore-former. *Mater. Lett.* 110, 152–155.
- Castelein, O., Soulestin, B., Bonnet, J.P., Blanchart, P., 2001. The influence of heating rate on the thermal behaviour and mullite formation from a kaolin raw material. *Ceram. Int.* 27.
- Emani, S., Uppaluri, R., Purkait, M.K., 2013. Preparation and characterization of low cost ceramic membranes for mosambi juice clarification. *Desalination* 317, 32–40.
- Emani, S., Uppaluri, R., Purkait, M.K., 2014. Microfiltration of oil-water emulsions using low cost ceramic membranes prepared with the uniaxial dry compaction method. *Ceram. Int.* 40, 1155–1164.
- Fu, J., He, Q., Liu, B., Zhang, J., Hu, B., 2010. Study in adsorption behavior of polymer on molecular sieves by surface and pore properties. *Colloids Surf., A* 369, 113–120.
- Gougazeh, M., Buhl, J.-C., 2014. Synthesis and characterization of zeolite A by hydrothermal transformation of natural Jordanian kaolin. *J. Assoc. Arab Univ. Basic Appl. Sci.* 15, 35–42.
- Han, Z., Tang, L.C., Xu, J., Li, Y., 2009. A three-parameter Weibull statistical analysis of the strength variation of bulk metallic glasses. *Scripta Mater.* 61, 923–926.
- Jana, S., Purkait, M.K., Mohanty, K., 2010. Preparation and characterization of low-cost ceramic microfiltration membranes for the removal of chromate from aqueous solutions. *Appl. Clay Sci.* 47, 317–324.
- Mauricio, V.L., Alves, O.L., Mazali, I.O., 2011. Macroporous glass monoliths prepared from powdered niobium phosphate glass by fast sintering. *Mater. Charact.* 62, 263–267.

- Naito, K., 2014a. Tensile properties and fracture behavior of different carbon nanotube-grafted polyacrylonitrile-based carbon fibers. *J. Mater. Eng. Perform.* 23, 3916–3925.
- Naito, K., 2014b. Tensile properties of polyimide composites incorporating carbon nanotubes-grafted and polyimide-coated carbon fibers. *J. Mater. Eng. Perform.* 23, 3245–3256.
- Nandi, B.K., Uppaluri, R., Purkait, M.K., 2008. Preparation and characterization of low cost ceramic membranes for micro-filtration applications. *Appl. Clay Sci.* 42, 102–110.
- Quinn, J.B., Quinn, G.D., 2010. A practical and systematic review of Weibull statistics for reporting strengths of dental materials. *Dental Mater.* 26, 135–147.
- Roos, M., Stawarczyk, B., 2012. Evaluation of bond strength of resin cements using different general-purpose statistical software packages for two-parameter Weibull statistics. *Dental Mater.* 28, e76–e88.
- Sahnoun, R.D., Baklouti, S., 2013. Characterization of flat ceramic membrane supports prepared with kaolin-phosphoric acid-starch. *Appl. Clay Sci.* 83–84, 399–404.
- Schmitt, M., Fernandes, C.P., da Cunha Neto, J.A.B., Wolf, F.G., dos Santos, V.S.S., 2013. Characterization of pore systems in seal rocks using nitrogen gas adsorption combined with mercury injection capillary pressure techniques. *Mar. Pet. Geol.* 39, 138–149.
- Yakub, I., Du, J., Soboyejo, W.O., 2012. Mechanical properties, modeling and design of porous clay ceramics. *Mater. Sci. Eng., A* 558, 21–29.